Available online at www.sciencedirect.com
SCIENCE DIRECT®
International Journal of Heat and Mass Transfer 48 (2005) 2117–2125
International Journal of HEAT and MASS TRANSFER
www.elsevier.com/locate/ijhmt

# Mixed convection heat transfer enhancement through film evaporation in inclined square ducts

Jer-Huan Jang [a], Wei-Mon Yan [b,*], Chien-Chang Huang [c]

[a] Department of Mechanical Engineering, Northern Taiwan Institute of Science and Technology, Pei-To, Taipei, Taiwan 112, PR China
[b] Department of Mechatronic Engineering, Huafan University, Shih Ting, Taipei, Taiwan 223, PR China
[c] Center for Environment Safety and Health Technology Development, Industrial Technology Research Institute, Chu Tung, Hsin Chu, Taiwan 310, PR China

Received 24 August 2004; received in revised form 31 December 2004
Available online 26 February 2005

**Abstract**

The investigation of mixed convection heat transfer enhancement through film evaporation in inclined square ducts has been numerically examined in detail. The main parameters discussed in this work include the inclined angle, the wetted wall temperature and the relative humidity of the moist air mixture. The numerical results of the local friction factor, Nusselt number and Sherwood number are presented for moist air mixture system. Attention was particular paid to the effects of latent heat transport on the heat transfer enhancement. Results show that the latent heat transport with film evaporation augments tremendously the heat transfer rate. The heat transfer rate can be enhanced to be 10 times of that without mass transfer, especially for a system with a lower temperature. Besides, better heat and mass transfer rates related with film evaporation are found for case with a higher wetted wall temperature. The increase in the relative humidity of moist air in the ambient causes the decrease in heat transfer enhancement.


## 1. Introduction

The mixed convection duct flows with coupled heat and mass transfer in a flowing gas mixture can be significantly affected by the combined buoyancy forces due to the existence of temperature and concentration variations. The understanding of the modification of flow structure in a duct is important in various engineering systems and environments, such as the solar energy collectors, design of heat exchangers, geothermal energy systems, chemical deposition of solid layer in the semiconductor industry, cooling of the nuclear reactor, modern electronic equipments, and thermo-protection systems from high temperature gas streams in supersonic aircraft and combustion chambers. Due to such widespread applications, mixed convection heat and mass transfer of gas mixture has received considerable attention.

For internal flows of mixed convection heat and mass transfer, the interactions of hydrodynamic, thermal and concentration development become fairly complicated. The effects of combined buoyancy forces of heat and mass diffusion on laminar mixed convection heat transfer in vertical and horizontal rectangular ducts were studied extensively. Yan [1] presented a numerical study

* Corresponding author. Tel.: +886 2 2663 2102; fax: +886 2 2663 2143.
*E-mail address:* wmyan@huafan.hfu.edu.tw (W.-M. Yan).

0017-9310/$ - see front matter © 2005 Elsevier Ltd. All rights reserved.
doi:10.1016/j.ijheatmasstransfer.2004.12.022

**Nomenclature**

| | |
|---|---|
| $a$ | width or height of a square duct (m) |
| $c$, $C$ | dimensional and dimensionless species concentration, respectively |
| $D$ | mass diffusivity ($m^2 s^{-1}$) |
| $f$ | friction factor, $2\bar{\tau}_w/(\rho_0 w_0^2)$ |
| $g$ | gravitational acceleration ($m s^{-2}$) |
| $Gr_T$ | heat transfer Grashof number, $g\beta(T_w - T_0)a^3/v^2$ |
| $Gr_M$ | mass transfer Grashof number, $g\beta^*(c_w - c_0)a^3/v^2$ |
| $\bar{h}$ | locally averaged heat transfer coefficient on the wetted wall ($W m^{-2} K^{-1}$) |
| $h_{fg}$ | latent heat of vaporization ($J kg^{-1}$) |
| $\bar{h}_m$ | locally averaged mass transfer coefficient on the wetted wall ($m s^{-1}$) |
| $k$ | thermal conductivity ($W m^{-1} K^{-1}$) |
| $M_a$ | molar weight of air |
| $M_v$ | molar weight of water vapor |
| $n$ | outward normal direction to the wetted wall |
| $Nu_l$ | local Nusselt number for latent heat transfer |
| $Nu_s$ | local Nusselt number for sensible heat transfer |
| $Nu_x$ | local total Nusselt number ($=Nu_s + Nu_l$) |
| $\bar{p}$ | cross-sectional mean pressure (kPa) |
| $\bar{P}$ | dimensionless cross-sectional mean pressure |
| $p'$ | perturbation term about mean pressure (kPa) |
| $P'$ | dimensionless perturbation pressure |
| $Pr$ | Prandtl number, $v\backslash\alpha$ |
| $p_w$ | saturated water vapor pressure on the wetted porous wall |
| $q_l$ | latent heat flux flowing into air stream ($W m^{-2}$) |
| $q_s$ | sensible heat flux flowing into air stream ($W m^{-2}$) |
| $q_x$ | interfacial total heat flux into air stream ($W m^{-2}$) |
| $Re$ | Reynolds number, $w_0 \cdot a/v$ |
| $S$ | parameter in Eq. (17) |
| $Sc$ | Schmidt number, $v$/D |
| $Sh$ | Sherwood number,$\bar{h}_m a/v$ |
| $T$ | temperature (K) |
| $U$, $V$, $W$ | dimensionless velocity components in the $X$, $Y$, $Z$ directions, respectively |
| $u$, $v$, $w$ | velocity components in the $x$, $y$, $z$ directions, respectively ($m s^{-1}$) |
| $X$, $Y$, $Z$ | dimensionless rectangular coordinate, $X = x/a$, $Y = y/a$, $Z = z/(Re \cdot a)$ |
| $Z^*$ | dimensionless $z$-direction coordinate, $z/(PrRe \cdot a) = Z/Pr$ |
| $x$, $y$, $z$ | rectangular coordinate system (m) |

*Greek symbols*

| | |
|---|---|
| $\alpha$ | thermal diffusivity ($m^2 s^{-1}$) |
| $\beta$ | coefficient of thermal expansion (1/K) |
| $\beta^*$ | coefficient of concentration expansion |
| $\delta$ | duct inclination angle |
| $\phi$ | relative humidity of moist in the ambient |
| $v$ | kinematic viscosity ($m^2 s^{-1}$) |
| $\xi$ | dimensionless vorticity in axial direction |
| $\rho$ | density ($kg m^{-3}$) |
| $\theta$ | dimensionless temperature, $(T - T_0)/(T_w - T_0)$ |

*Superscript*

| | |
|---|---|
| – | average quantity |

*Subscripts*

| | |
|---|---|
| b | bulk fluid quantity |
| m | caused by mass |
| 0 | condition at inlet |
| w | condition at the duct wall |

of mixed convection heat and mass transfer in a horizontal rectangular duct. He found that the heat and mass transfer are enhanced as the buoyancy force from species diffusion assists the thermal buoyancy force. Cheng and Hwang [2] experimentally studied the effect of mass injection on laminar flow and heat transfer characteristics in a horizontal one-porous-wall square duct. They concluded that a larger friction factor and a smaller heat transfer rate resulted from a larger injection rate. Lee et al. [3] numerically investigated the mixed convection heat and mass transfer in vertical ducts. Their results show that the influences of the combined buoyancy force of thermal and mass diffusion on the flow, heat and mass transfer are significant.

As far as convection heat and mass transfer with film evaporation concerned, investigations on mixed convection heat and mass transfer with film evaporation in inclined ducts have not been adequately studied. Chow and Chung [4] have studied on the evaporation of water film into a gas stream along a flat plate. They focused on heat and mass transfer in a gas stream by assuming the liquid film to be extremely thin and found that mass transfer associated with the film evaporation has a pronounced impact on the heat transfer. Recently, Hammou et al. [5] have numerically studied the effect of simultaneous cooling and mass transfer on laminar flow of humid air in a vertical channel. They found that cooling of the hot humid air is accompanied by either con-

densation or evaporation. Debbissi et al. [6] analyzed the evaporation of water into humid air and superheated steam. In their work, particular attention is paid to study the effect of the ambient conditions on evaporation rate of water and the inversion temperature of the phenomenon in the condition of free and mixed convection.

Yan et al. [7–11] and Fedorov et al. [12] investigated the influences of wetted wall on laminar or turbulent mixed convection heat and mass transfer in vertical channels. The results showed that the effects of the evaporation of water vapor on the heat transfer are rather substantial. Boukadida and Nasrallah [13] numerically examined forced convection heat and mass transfer in vertical rectangular duct with film evaporation. In this work, they only considered the evaporation effects and neglected the buoyancy effects. As for the studies on the mixed convection heat and mass transfer in rectangular ducts, Lin et al. [14] presented a pioneer study. In Ref. [14], Lin et al. considered the combined buoyancy effects resulting from the thermal and mass buoyancies on the forced convection in a horizontal duct.

However, different orientations of the channel can induce different kinds of thermal buoyant flows which enhance the heat transfer in different manners. For inclined ducts, buoyancy forces act in both main flow and the cross-stream directions. In fact, the buoyancy forces can be decomposed into two components: one normal to and another parallel with the forced flow. Yan [15] has studied numerically on the transport phenomena of mixed convection heat and mass transfer in an inclined rectangular duct. He found that the buoyancy forces distort the velocity, temperature and concentration distributions. But in his study [15], the film evaporation effects are not taken into account. Huang and Lin [16] investigated the transient mixed convection air flow in a bottom heated inclined rectangular duct. Their attention was particularly paid to delineate the effects of the duct inclination and thermal buoyancy on the flow transition.

It is noted from the paper review cited above, despite its practical importance, that studies of mixed convection heat and mass transfer in inclined ducts with film evaporation has not received sufficient attention. This motivates the present investigation. In present work, an attempt is made to examine the heat transfer enhancement through the transport of latent heat on mixed convection heat and mass transfer in inclined square ducts.

## 2. Analysis

Consider a steady three-dimensional laminar upward flow of moist air mixture in the entrance region of a square duct inclined at an angle of $\delta$ to the horizontal,

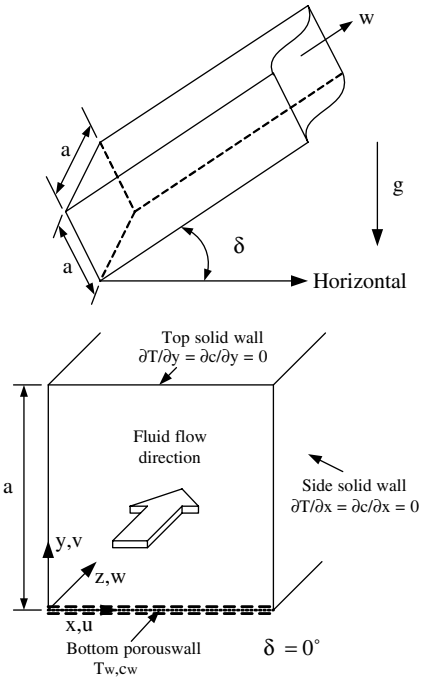


Fig. 1. Schematic diagram of the physical system.

as schematically shown in Fig. 1. The width or height of the square duct is $a$. The bottom porous wall of the duct is wetted by the thin liquid film and maintained at a constant temperature, $T_w$. The other walls of the duct are insulated solid walls. The $u$, $v$ and $w$ are the velocity components in the $x$, $y$ and $z$ directions, respectively. The air–water mixture entering into the duct has a constant axial velocity $w_0$, temperature $T_0$, concentration $c_0$, and relative humidity $\phi$.

The problem to be analyzed is the heat and mass transfer for simultaneously developing laminar flow with combined buoyancy effects of thermal and mass diffusion in an inclined square duct. Due to the symmetric inherent in this problem, the calculations can be restricted to a solution domain that comprises one-half of the inclined square duct. The thermo-physical properties of the mixture are assumed to be constant and evaluated by the one-third rule [17] except for density variations in the buoyancy term in the $y$- and $z$-direction momentum equations and obedient to the Boussinesq approximation. The liquid film on the porous wall is assumed to be thin enough that can be treated as a boundary condition in order to simplify the analysis. The flow is assumed to be parabolic and in the $z$-direction momentum equation a space-averaged pressure $\bar{p}$ is imposed to prevail at each cross-section, permitting a decoupling of the pressure in the cross-sectional momentum equation. The dynamic pressure can be presented as the sum of a cross-sectional mean pressure $\bar{p}(z)$, which

derives the main flow and a perturbed pressure about the mean, $p'(x,y)$, which derives the cross-stream flow. The 'pressure uncoupling' follows the parabolic-flow practice and, together with the neglect of axial diffusion momentum, heat and concentration by an order of analysis, permits a marching-integration calculation procedure.

The governing equations are those of conservation of mass, momentum, energy and concentration. By introducing the following the dimensionless variables,

$$X=\frac{x}{a};\quad Y=\frac{y}{a};\quad Z=\frac{z}{Re\cdot a};\quad U=\frac{ua}{v};\quad V=\frac{va}{v};$$
$$W=\frac{w}{w_0}$$
$$\overline{P}=\frac{\overline{p}}{\rho_0 w_0^2};\quad P'=\frac{p'a^2}{\rho_0 v^2};\quad \theta=\frac{T-T_0}{T_w-T_0};\quad c=\frac{c-c_0}{c_w-c_0};$$
$$Z^*=\frac{Z}{Pr}$$
$$Re=\frac{w_0 a}{v};\quad Pr=\frac{v}{\alpha};\quad Sc=\frac{v}{D};\quad Gr_T=\frac{g\beta(T_w-T_0)a^3}{v^2};$$
$$Gr_M=\frac{g\beta^*(c_w-c_0)a^3}{v^2} \tag{1}$$

and adopting the assumptions made earlier and the vorticity–velocity formulation developed by Ramakrishna et al. [18], the non-dimensional governing equations can be obtained as follows:

$$\frac{\partial^2 U}{\partial X^2}+\frac{\partial^2 U}{\partial Y^2}=\frac{\partial \xi}{\partial Y}-\frac{\partial^2 W}{\partial X\,\partial Z} \tag{2}$$

$$\frac{\partial^2 V}{\partial X^2}+\frac{\partial^2 V}{\partial Y^2}=-\frac{\partial \xi}{\partial X}-\frac{\partial^2 W}{\partial Y\,\partial Z} \tag{3}$$

$$U\frac{\partial \xi}{\partial X}+V\frac{\partial \xi}{\partial Y}+W\frac{\partial \xi}{\partial Z}+\xi\left(\frac{\partial U}{\partial X}+\frac{\partial V}{\partial Y}\right)+\left(\frac{\partial W}{\partial Y}\cdot\frac{\partial U}{\partial Z}-\frac{\partial W}{\partial X}\cdot\frac{\partial V}{\partial Z}\right)=\frac{\partial^2 \xi}{\partial X^2}+\frac{\partial^2 \xi}{\partial Y^2}-\cos\delta\left(Gr_T\frac{\partial \theta}{\partial X}+Gr_M\frac{\partial C}{\partial X}\right) \tag{4}$$

$$U\frac{\partial W}{\partial X}+V\frac{\partial W}{\partial Y}+W\frac{\partial W}{\partial Z}=-\frac{d\overline{P}}{dZ}+\frac{\partial^2 W}{\partial X^2}+\frac{\partial^2 W}{\partial Y^2}+\sin\delta(Gr_T\cdot\theta+Gr_M\cdot C) \tag{5}$$

$$U\frac{\partial \theta}{\partial X}+V\frac{\partial \theta}{\partial Y}+W\frac{\partial \theta}{\partial Z}=\frac{1}{Pr}\left(\frac{\partial^2 \theta}{\partial X^2}+\frac{\partial^2 \theta}{\partial Y^2}\right) \tag{6}$$

$$U\frac{\partial C}{\partial X}+V\frac{\partial C}{\partial Y}+W\frac{\partial C}{\partial Z}=\frac{1}{Sc}\left(\frac{\partial^2 C}{\partial X^2}+\frac{\partial^2 C}{\partial Y^2}\right) \tag{7}$$

Because of the symmetric characteristics shown in Fig. 1, the corresponding boundary conditions could be given as entrance ($Z=0$)

$$W=1;\ U=V=\xi=\theta=C=0 \tag{8a}$$

Symmetric plane ($X=1/2$)

$$\frac{\partial W}{\partial X}=U=\frac{\partial V}{\partial X}=\frac{\partial \theta}{\partial X}=\frac{\partial C}{\partial X}=0 \tag{8b}$$

duct walls

$$U=V=W=0;\quad \frac{\partial \theta}{\partial X}=\frac{\partial C}{\partial X}=0 \text{ at } X=0 \tag{8c}$$

$$U=W=0;\ V=V_w;\quad C=1;\ \theta=1 \text{ at } Y=0 \tag{8d}$$

$$U=V=W=0;\quad \frac{\partial \theta}{\partial Y}=\frac{\partial C}{\partial Y}=0 \text{ at } Y=1 \tag{8e}$$

Because the bottom wetted wall is porous and semi-permeable (the solubility of air in water is negligibly small and air velocity in the $y$-direction is stationary at the interface), the evaporating velocity of the mixture on the wetted wall can be evaluated by the following equation [19,20],

$$V_w=-\frac{(c_w-c_0)}{Sc(1-c_w)}\frac{\partial C}{\partial Y} \tag{9}$$

According to the Dalton's law and the state equation of ideal gas mixture, the interfacial mass fraction of water vapor on the wetted wall can be calculated by

$$c_w=\frac{p_w M_v}{p_w M_v+(p-p_w)M_a} \tag{10}$$

where $p_w$ is the saturated water vapor pressure on the wetted wall.

One constraint to be satisfied is that the overall mass flow rate at every axial location must be balanced in the duct flow, which is used to deduce the axial pressure gradient in axial momentum equation. This constrain can be expressed as follow:

$$\int_0^1\int_0^{\frac{1}{2}} W\,dX\,dY=\frac{1}{2}+\int_0^Z\int_0^{\frac{1}{2}} V_w\,dX\,dZ \tag{11}$$

The local friction coefficient is defined to be $f=\frac{2\bar{\tau}_w}{\rho w_0^2}$, where $\bar{\tau}_w$ is the peripherally averaged shear stress and $w_0$ stands for the inlet average axial velocity. Following the usual definitions and using the dimensionless variables, the expression for the product of the peripherally averaged friction factor and Reynolds number can be expressed as

$$fRe=-2\left.\frac{\overline{\partial W}}{\partial n}\right|_{wall} \tag{12}$$

Energy transport between the wetted wall and the fluid in the duct in the presence of mass transfer depends on two factors: (1) the fluid temperature gradient at the wetted wall, resulting in a sensible heat transfer; (2) the rate of mass transfer, resulting in a latent heat transfer. Therefore, the total heat flux from the wetted wall can be expressed as:

$$q_x = q_s + q_l = -k\left.\frac{\partial T}{\partial y}\right|_{y=0} - \frac{\rho D h_{fg}}{1-c_w}\cdot\left.\frac{\partial c}{\partial y}\right|_{y=0} \quad (13)$$

The locally averaged heat transfer coefficient on the wetted wall, $\bar{h}$ , which relates to the supply of heat flux from the heated porous wall, may be defined as $\bar{h} = \frac{q_x}{T_w - T_b}$ . Therefore, the locally averaged Nusselt numbers along the wetted surface is defined as

$$Nu_x = \frac{\bar{h}a}{k} = \frac{q_x a}{k(T_w - T_b)} = Nu_s + Nu_l \quad (14)$$

where $Nu_s$ and $Nu_l$ are the local Nusselt numbers for sensible and latent heat transfer, respectively, and they are defined as the following:

$$Nu_s = \frac{-1}{1-\theta_b}\left.\frac{\overline{\partial\theta}}{\partial Y}\right|_{Y=0} \quad (15a)$$

$$Nu_l = \frac{-S}{1-\theta_b}\cdot\frac{1}{1-c_w}\left.\frac{\overline{\partial C}}{\partial Y}\right|_{Y=0} \quad (15b)$$

where $S$ indicates the importance of the energy transport through species diffusion relative to that through thermal diffusion [21],

$$S = \frac{\rho D h_{fg}(c_w - c_0)}{k(T_w - T_0)} \quad (16)$$

For a low mass transfer rate at the interface, the locally averaged Sherwood number on the wetted wall can be formulated as

$$Sh = \frac{\bar{h}_m a}{D} = \frac{-1}{1-C_b}\left.\frac{\overline{\partial C}}{\partial Y}\right|_{Y=0} \quad (17)$$

In Eq. (15), the bulk fluid temperature $\theta_b$ and bulk fluid concentration $C_b$ are defined as

$$\theta_b = \frac{\int_0^1\int_0^{\frac{1}{2}}\theta\cdot W\,dX\,dY}{\int_0^1\int_0^{\frac{1}{2}}W\,dX\,dY}; \quad C_b = \frac{\int_0^1\int_0^{\frac{1}{2}}C\cdot W\,dX\,dY}{\int_0^1\int_0^{\frac{1}{2}}W\,dX\,dY} \quad (18)$$

## 3. Numerical approach

In present work, the governing equations are solved by the vorticity–velocity method for three-dimensional parabolic flow [18] for the velocities, temperature and concentration. The detailed numerical method and solution procedure are available in Ref. [15] and are not presented here. In the present study, the uniform cross-sectional meshes were chosen, while the $z$-direction grid spacing was non-uniform with grid lines being more closely packed near the entrance. The axial step size $\Delta Z$ was varied from $2\times10^{-6}$ near the duct entrance to about $2\times10^{-3}$ near the fully-developed region. In the program test, a finer axial step size was tried and found to give acceptable accuracy. Furthermore, as a partial verification of the computation procedure, results were initially obtained for mixed convection heat transfer in an inclined rectangular duct without film evaporation. The results are compared with those of Yan [15]. The Nusselt numbers were found to agree within 3%. Through these program tests, the solution method and the formulation adopted are appropriate for the present study.

## 4. Results and discussion

The development of velocity, temperature and concentration profiles are of engineering interest and useful in clarifying the heat and mass transfer mechanism. However, the major goal in this work is to investigate the heat transfer enhancement through the transport of latent heat in an inclined square duct. Therefore, the axial developments of velocity, temperature and concentration profiles are not shown in this work for the reason of limited space available for the article. In this study, the incoming air mixture at the inlet is fixed at 20 °C and 1 atm, the inlet relative humidity is chosen to be 10%, 30%, 50%, 70% or 90%, the wetted wall is kept at a uniform temperature being 30, 40, 50 or 60 °C, the through-flow Reynolds number at the inlet is assigned to be 1000, and the inclination angle is set to be 30°, 45°, 60°, 75° or 90°. The typical case is set for 40 °C of the wetted wall temperature, 50% of the inlet relative humidity with 45° of inclination. Table 1 presents the dimensional parameters used in this work and their corresponding non-dimensional governing parameters.

### 4.1. Effects of duct inclination angles

In order to illustrate the effects of the duct inclination on the heat transfer, friction factor and mass transfer, results for various inclination angles are presented in Figs. 2 and 3. The axial distributions of sensible and total Nusselt numbers are shown in Fig. 2(a) and (b), respectively. The 0° inclination indicates the flow in a

Table 1
Parameters used in this work

| $T_w$ (°C) | $\theta$ (%) | $Gr_T$ | $Gr_M$ | $S$ | $Pr$ | $Sc$ |
|---|---|---|---|---|---|---|
| 30 | 50 | 21508 | 7387 | 5.39 | 0.706 | 0.594 |
| 40 | 50 | 40054 | 14058 | 5.39 | 0.703 | 0.592 |
| 50 | 50 | 56248 | 24139 | 6.42 | 0.701 | 0.588 |
| 60 | 50 | 70687 | 39378 | 8.06 | 0.701 | 0.583 |
| 40 | 10 | 40010 | 16102 | 6.19 | 0.703 | 0.592 |
| 40 | 30 | 40032 | 15082 | 5.79 | 0.703 | 0.592 |
| 40 | 70 | 40076 | 13029 | 4.99 | 0.703 | 0.591 |
| 40 | 90 | 40098 | 11995 | 4.59 | 0.703 | 0.591 |

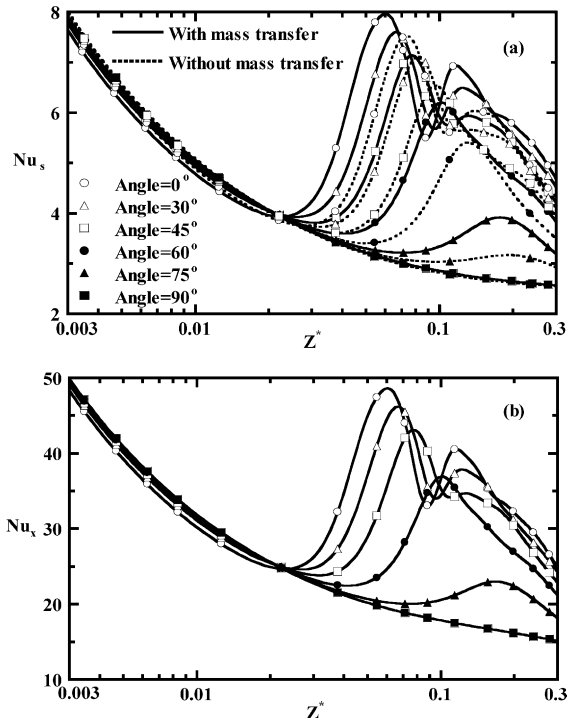


Fig. 2. Effects of inclination angle on local distributions of (a) sensible heat Nusselt number and (b) total Nusselt number.

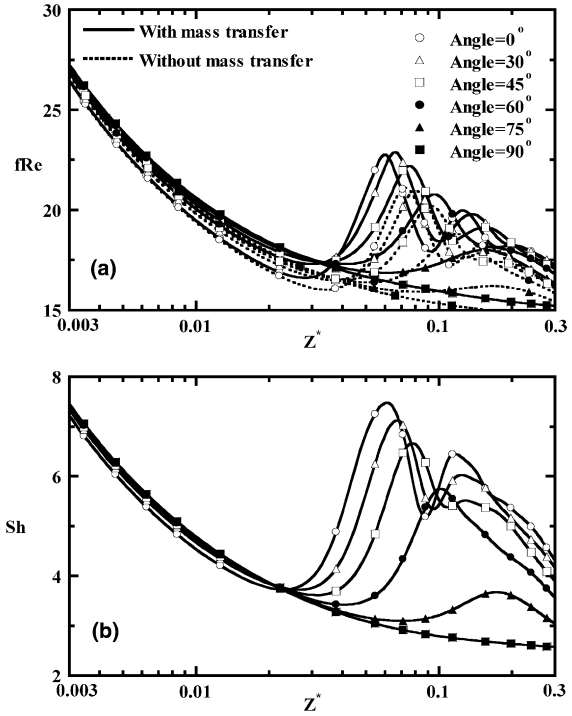


Fig. 3. Effects of inclination angle on local distributions of (a) friction factor and (b) Sherwood number.

horizontal duct, while 90° stands for the flow in a vertical duct. It is shown that both sensible and total heat transfer rates decrease near the entrance, which is known to be the forced-convection effect. It is noted that all the curves near the entrance seem to coincide with each other. After a certain axial location, both the sensible and latent heat transfer rates deviate from the forced convection results due to the formation of the secondary flows, except for the case with 90°. For the mixed convection duct flows, there are two components of the buoyancy forces: normal and parallel to the forced flow in an inclined duct. For a larger inclination angle measured from horizontal, the normal buoyancy force decreases while the parallel buoyancy force accelerated the flow increases. At the entrance, the forced flow is dominant and parallel buoyancy force increases as inclination angle increases. The buoyancy force with less inclination angle is larger after a specific distance from the entrance which depends on the value of inclination angle that causes a higher heat transfer rate. It is also seen that the Nusselt number with mass transfer is always larger than that without mass transfer. This is because the buoyancy force caused by mass transfer is enhanced due to the film evaporation. It is clear that the trends of sensible and total heat transfer rates are similar. From Eq. (14), the latent heat transfer is the difference of total and sensible heat transfer. Therefore, the value of sensible heat transfer is an order less than that of latent heat transfer. It reveals that the heat transfer duo to latent heat transport associated with film evaporation is much more effective than that due to sensible heat transfer connected to the temperature difference.

The axial distributions of friction factor and Sherwood number with and without mass transfer are illustrated in Fig. 3(a) and (b), respectively. It is observed in Fig. 3(a) that near the entrance, the friction factor decreases as the flow moves downstream. After a certain axial location, the friction factor begins to increase. For a smaller inclination angel, the friction factor has more than one maximum value. This is due to the developments of successive strengthening and weakening of the secondary flow being repeated. The occurrence of maximum local friction factor is closely related to the appearance of local maximum secondary flow intensity. It is seen that the friction factor increases with the inclination angle near the entrance. It is also depicted that the friction factor with mass transfer is always larger than that without mass transfer. This is understandable that when mass buoyancy due to mass transfer will assist the main flow, which in turn, cause an increase in the friction factor. The mass transfer shown in Fig. 3(b) has similar profile to the sensible heat transfer in Fig. 2(a). However the value of sensible Nusselt number is larger than that of Sherwood number. This is owing to the fact that the Prandtl number is larger than the Schmidt number for the moist air mixture.

### 4.2. Wetted wall temperature effect

The effects of wetted wall temperature $T_w$ on the sensible and total Nusselt numbers are presented in Fig. 4(a) and (b), respectively. A higher wetted wall temperature results in a larger sensible heat transfer. This is expected because the larger combined buoyancy is for a system with a higher wetted wall temperature. It is noted that the buoyancy effect is negligible up to a certain axial distance depending on the wetted wall temperature. As the wetted wall temperature is raised, the distance from the inlet becomes shorter. Again, it is also found that the sensible heat transfer with consideration of the mass transfer effects is always larger than that without mass transfer for a fixed wetted wall temperature. The effect of wetted wall temperature on the total heat transfer is presented in Fig. 3(b). It is clearly seen that better heat transfer rate is noted for a system with a higher wetted wall temperature. This can be made plausible by noting the fact that the higher the wetted wall temperature is, the better the latent heat transport related with the liquid film evaporation is. Comparison of the magnitude in the $Nu_s$ and $Nu_x$ indicates that the heat transfer resulting from the latent heat transport is much more effective.

The effects of wetted wall temperature on the local friction factor and Sherwood number are shown in Fig. 5(a) and (b), respectively. It is observed that the local friction factor increases as the wetted wall temperature increases. This is because a higher wetted wall temperature will increase a larger film evaporation rate on the wetted wall, which in turn, causes the larger aiding buoyancy forces to the main flow. In Fig. 5(b), the distributions of Sherwood numbers resemble those of $Nu_s$ in Fig. 4(a). This is because the $Pr$ and $Sc$ are of the same order of magnitude. It is also found that the local Sherwood number increases as the wetted wall temperature increases. This is due to the larger combined buoyancy forces for a system with a higher wall temperature.

### 4.3. Effects of inlet relative humidity

The effect of inlet humidity and wetted wall temperature are of interest in understanding the heat transfer mechanism by the transport of latent heat exchange. Fig. 6 presents the effects of the relative humidity of moist air and wetted wall temperature on the average friction factor and total Nusselt number. The overbar means the averaged value of longitudinal values from the entrance to the downstream ($Z^* = 0.3$). From Fig. 6(a), it is clearly seen that the averaged friction factor increases with an increase in the wetted wall temperature. This is due to the fact that the combined thermal and

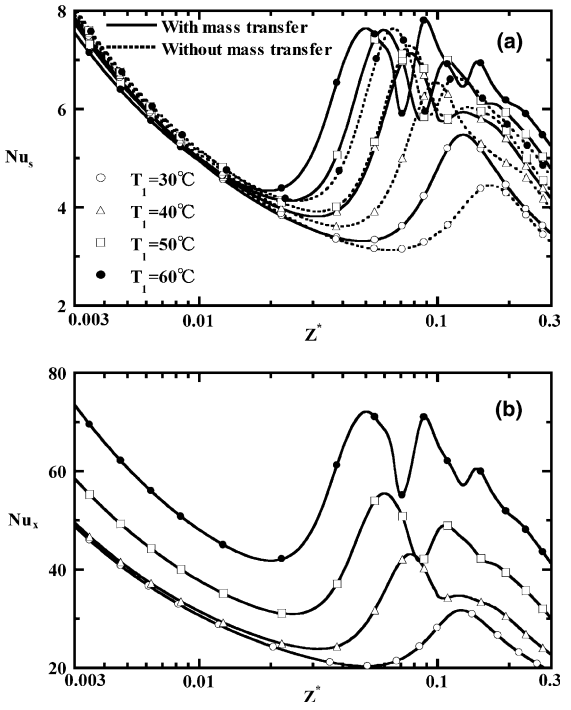


Fig. 4. Effects of wetted wall temperature on local distributions of (a) sensible heat Nusselt number and (b) total Nusselt number.

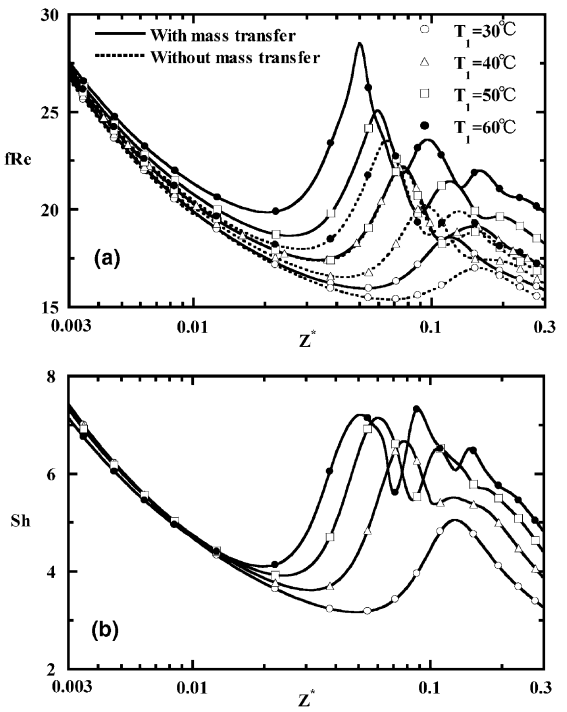


Fig. 5. Effects of wetted wall temperature on local distributions of (a) friction factor and (b) Sherwood number.

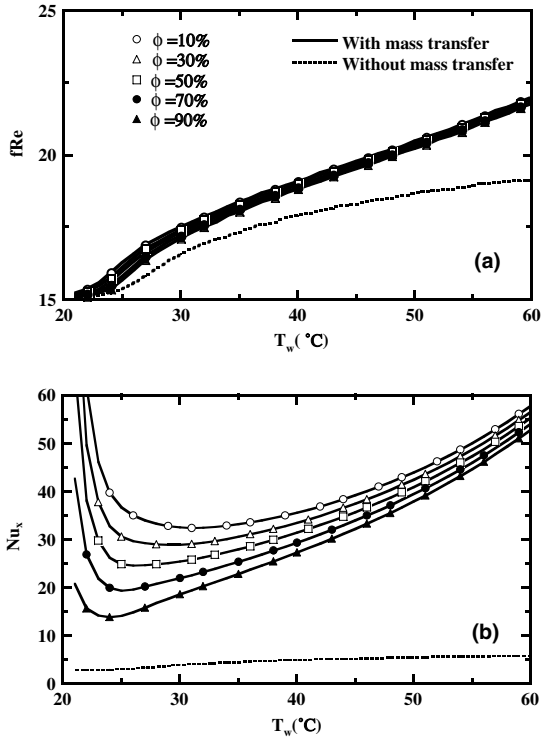


Fig. 6. Effects of inlet relative humidity and wetted wall temperature on (a) average friction factor and (b) average Nusselt number.

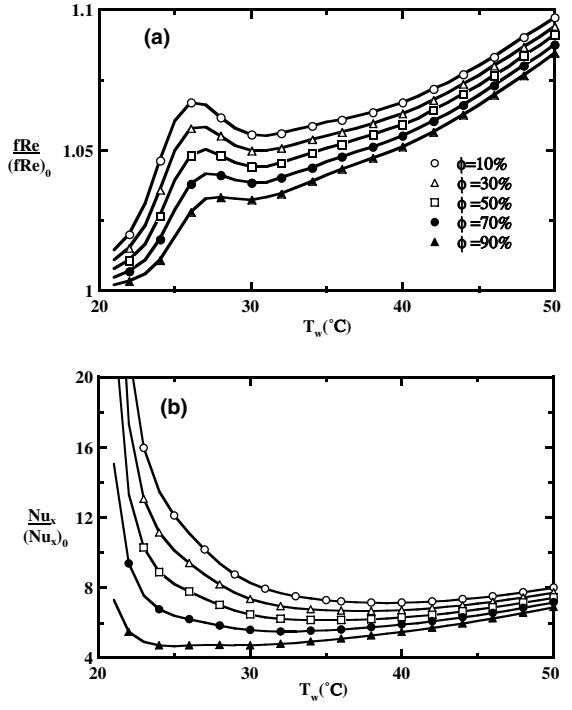


Fig. 7. Effects of inlet relative humidity and wetted wall temperature on (a) friction factor ratio and (b) Nusselt number ratio.

mass buoyancy forces are stronger for a higher wetted wall temperature. Besides, the averaged friction factor with mass transfer is larger than that without mass transfer owing to the additional mass buoyancy force. Although the effects of relative humidity on the average friction factor are not significant, their effects on the heat transfer are considerable. In Fig. 6(b), the lower the relative humidity is, the higher the heat transfer rate is. This can be made plausible by noting that the total heat transfer on the wetted wall is the sum of the sensible and latent heat transfer rates. The latent heat transfer is related to the film evaporation which is much more significant under the condition of lower relative humidity of mist air.

It is interesting to examine the effects of relative humidity and wetted temperature on the enhancement in the friction factor and heat transfer. Therefore, the curves in Fig. 6 are re-drawn to exhibit the effects of the augmentation in friction factor and Nusselt number. Fig. 7 presents the effects of the relative humidity of moist air and wetted wall temperature on the average friction factor ratio and total Nusselt number ratio. The subscript o denotes the quantity for the case without mass transfer. Therefore, the values of friction factor ratio and Nusselt number ratio indicate the enhancement due to the mass transfer. An overall inspection on Fig. 7 discloses that the values of the friction factor ratio are less than 1.1. This means that the increase in the friction factor due to mass transfer is less 10%. But, for the Nusselt number ratio, the values can reach 10, especially for the case with lower wetted temperature and relative humidity. This implies that the heat transfer enhancement in association with the film evaporation is very effective. This suggests that the heat transfer enhancement through film evaporation is appropriate in the design of heat transfer enhancement. A careful examination of Fig. 7 shows that the friction factor ratio decreases at the wall temperature between 26 and 30 °C. In addition, a higher inlet relative humidity results in a lower friction factor ratio. This can be explained by the fact that more film evaporates as the inlet relative humidity is lower, which causes stronger mass buoyancy force effect. It is observed in Fig. 7(b) that the heat transfer enhancement decreases and then increases as the wetted wall temperature increases. It is also found that a lower heat transfer enhancement is resulted from a higher inlet relative humidity. This is owing to the fact that the heat transfer on the wetted wall is strongly affected by the film evaporation related to the species diffusion. For the evaporative mass transfer, the species diffusion mechanism is more effective at lower concentration levels.

## 5. Conclusions

The problem of mixed convection heat transfer enhancement through film evaporation in inclined square ducts has been analyzed. The effects of inclination angel, wetted wall temperature, and inlet relatively humidity on momentum, heat and mass transfer have been studied in detail. Brief summaries of the major results are listed in the following:

1. The friction factor, heat and mass transfer are affected considerably by the inclination angle of the duct, especially for a lower inclination angle.
2. Heat transfer duo to latent heat transport associated with film evaporation is much more effective than that due to sensible heat transfer connected to the temperature difference.
3. Better heat and mass transfer rates related with film evaporation are found for a system with a lower relative humidity of moist air or a higher wetted wall temperature.
4. The heat transfer rate can be enhanced to be 10 times of that without mass transfer, especially for a system with a lower temperature.

## Acknowledgement

The authors would like to acknowledge the financial support of the present work by NSC and ITRI. The financial support from Northern Taiwan Institute of Science and Technology is also acknowledged.

## References

[1] W.M. Yan, Combined buoyancy effects of thermal and mass diffusion on laminar forced convection in horizontal rectangular ducts, Int. J. Heat Mass Transfer 39 (1996) 1479–1488.
[2] Y.C. Cheng, G.J. Hwang, Experimental studies of laminar flow and heat transfer in a one-porous-wall square duct with wall injection, Int. J. Heat Mass Transfer 38 (1995) 3475–3484.
[3] K.T. Lee, H.L. Tsai, W.M. Yan, Mixed convection heat and mass transfer in vertical rectangular ducts, Int. J. Heat Mass Transfer 40 (1997) 1621–1631.
[4] L.C. Chow and J.N. Chung, Water evaporation into a turbulent stream of air, humid air or superheated steam, Twenty-first ASME/AIChE National Heat Transfer Conference, Seattle, WA, ASME Paper no. 83-HT-2, 1983.
[5] Z.A. Hammou, B. Benhamou, N. Galanis, J. Orfi, Laminar mixed convection of humid air in a vertical channel with evaporation or condensation at the wall, Int. J. Therm. Sci. 43 (2004) 531–539.
[6] C. Debbissi, J. Orfi, S.B. Nasrallah, Evaporation of water by free or mixed convection into humid air and superheated steam, Int. J. Heat Mass Transfer 46 (2003) 4703–4715.
[7] T.F. Lin, C.J. Chang, W.M. Yan, Analysis of combined buoyancy effects of thermal and mass diffusion on laminar forced convection heat transfer in a vertical tube, ASME J. Heat Transfer 110 (1988) 337–344.
[8] W.M. Yan, Y.L. Tsay, T.F. Lin, Simultaneous heat and mass transfer in laminar mixed convection flows between vertical parallel plates with asymmetric heating, Int. J. Heat Fluid Flow 10 (1989) 262–269.
[9] W.M. Yan, T.F. Lin, Effects of wetted wall on laminar mixed convection heat transfer in a vertical channel, J. Thermophys. Heat Transfer 3 (1989) 94–96.
[10] W.M. Yan, Mixed convection heat transfer enhancement through latent heat transport in vertical parallel plate channel flows, Can J. Chem. Eng. 69 (1991) 1277–1282.
[11] W.M. Yan, Turbulent mixed convection heat and mass transfer in a wetted channel, ASME J. Heat Transfer 117 (1995) 229–233.
[12] A.G. Fedorov, R. Viskanta, A.A. Mohamad, Turbulent heat and mass transfer in an asymmetrically heated, vertical parallel-plate channel, Int. J. Heat Fluid Flow 18 (1997) 307–315.
[13] N. Boukadida, S.B. Nasrallah, Mass and heat transfer during evaporation in laminar flow inside a rectangular channel-validity of heat and mass transfer analogy, Int. J. Therm. Sci. 40 (2001) 67–81.
[14] J.N. Lin, P.Y. Tzeng, F.C. Chow, W.M. Yan, Convective instability of heat and mass transfer for laminar forced convection in the thermal entrance region of horizontal rectangular channels, Int. J. Heat Fluid Flow 13 (1992) 250–258.
[15] W.M. Yan, Transport phenomena of developing laminar mixed convection heat and mass transfer in inclined rectangular ducts, Int. J. Heat Mass Transfer 38 (1995) 2905–2914.
[16] C.C. Huang, T.F. Lin, Numerical simulation of transitional aiding mixed convection air flow in a bottom heated inclined rectangular duct, Int. J. Heat Mass Transfer 39 (1996) 1697–1710.
[17] T. Fujji, Y. Kato and K. Mihara, Expression of transport and thermodynamic properties of air, steam and water, Report No. 66, Department of Production Science, Kyushu University, Kyushu, Japan, 1977.
[18] K. Ramakrishna, S.G. Rubin, P.K. Khosla, Laminar natural convection along vertical square ducts, Numer. Heat Transfer 5 (1982) 59–79.
[19] L.C. Burmeister, Convective Heat Transfer, McGraw-Hill, New York, 1983, pp. 170–174.
[20] R.B. Bird, W.E. Stewart, E.N. Lightfood, Transport Phenomena, Wiley, New York, 1960.
[21] W.M. Yan, Effects of film evaporation on laminar mixed convection heat and mass transfer in a vertical channel, Int. J. Heat Mass Transfer 35 (1992) 3419–3429.